Paper 37

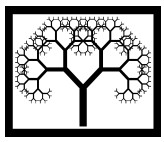

©Civil-Comp Press, 2012
Proceedings of the Eleventh International Conference
on Computational Structures Technology,
B.H.V. Topping, (Editor),
Civil-Comp Press, Stirlingshire, Scotland

A Finite Element for Bending Analysis of Sandwich Composite Beams

P. Belbute[1], A.L. Araújo[1], S. Teixeira de Freitas[2] and M. de Freitas[3]
[1] IDMEC/IST, Instituto Superior Tecnico
Technical University of Lisbon, Portugal
[2] Delft University of Technology, The Netherlands
[3] ICEMS, Instituto Superior Tecnico
Technical University of Lisbon, Portugal

Abstract

Nowadays, the use of composite laminated structures in the automobile, railroad, civil, aeronautical, space and naval industries is growing at a huge rate. Recently, there has been a renewed interest in sandwich laminated structures, whose bending capability and performance is much better when compared to classical laminates. Sandwich structures, which are mainly used as bending components, are formed by materials with very different stiffness in the faces and in the core. Therefore the behaviour of such structures under bending conditions does not fit the classical laminate theories. Despite this, sandwich structures are simple enough to allow simplified analysis, whose mathematical accuracy depends greatly on the structure itself. In this paper the goal is to study and validate the application in bending of a developed sandwich beam element with transverse compressibility of the core. This element uses a mixed layerwise approach by considering a higher-order shear deformation theory (HSDT) to represent the displacement field of the core and a first-order shear deformation theory (FSDT) for the face layers. Results are compared with three-dimensional finite element solutions and validation is also conducted with values retrieved experimentally.

Keywords: sandwich beams, beam elements, four point bending tests, validation.

1 Introduction

Sandwich structures are formed by two exterior faces which are relatively thin but of high structural stiffness and a thicker core, which is lighter but less stiff than the faces. The faces and core are usually bonded using adhesives.

There are many ways to combine materials for the construction of sandwich structures. This allows for optimization in accordance with the needs in engineering projects. In the faces the most used materials are steel, aluminium, wood, and laminated com-

posites of carbon fibres, fibreglass, etc. In the core, cork, balsa, polymeric foams such as polyurethane, polystyrene, phenolic resin, metallic or carbon honeycombs, among others, are the most used materials [1, 2].

Nowadays sandwich structures can be found in many different industries. In civil engineering applications the interest in these structures has been increasing, namely in the renovation of steel bridge decks. Due to fatigue problems the old decks of these bridges need to be replaced with a new Sandwich Plate System (SPS) [3, 4, 5].

Sandwich panels and beams are therefore simple structures with much better performance than classical laminates under bending conditions. They can be analysed using simple structural kinematics, although they are formed by a flexible core which does not allow the use of conventional beam and plate theories. Because of this, the need to use specific sandwich beam and plate models arises.

The main goal of this paper will be centred in the validation of a new beam finite element model, with transverse compressibility of the core, formulated using a mixed layerwise approach, by considering a Higher-Order Shear Deformation Theory (HSDT) to represent the displacement field of the viscoelastic core and a First-Order Shear Deformation Theory (FSDT) for the displacement field of the face layers. Four point bending results will then be compared with solutions obtained by 3D finite element analysis and validated using experimental results in accordance with ASTM regulations [6]. Because of their importance in sandwich structures, longitudinal and shear strains distributions will also be presented.

2 Hybrid sandwich beam model

The development of a layerwise sandwich beam finite element model is presented here. The basic assumptions in the development of the sandwich beam model of Figure 1 are:

- No slip occurs at the interfaces between layers;
- The displacement is C^0 along the interfaces;
- Elastic layers are modeled with first order shear deformation theory (FSDT) and viscoelastic core with a higher order shear deformation theory (HSDT);
- All materials in the core are linear, homogeneous and orthotropic and the elastic layers (faces) are made of laminated composite materials;

The present model is similar to the plate model presented by Araújo et al. [7], but including transverse compressibility of the core, which should be a significant effect for soft core sandwiches.

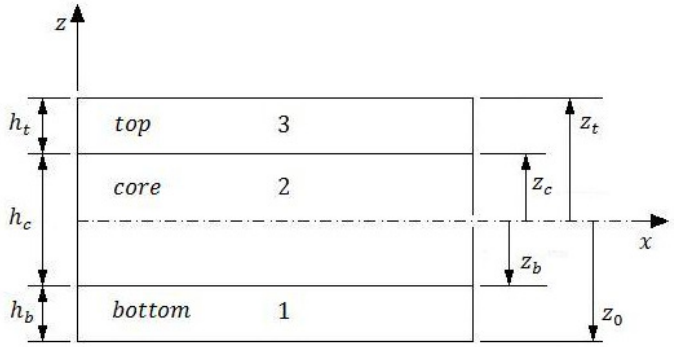

Figure 1: Sandwich beam model.

2.1 Displacement field

The FSDT displacement field of the face layers may be written in the general form:

$$\begin{aligned} u^k(x,y,z,t) &= u_0^k(x,t) + (z-\bar{z}_k)\theta_x^k(x,t) \\ w^k(x,y,z,t) &= w_0^k(x,t) \end{aligned} \tag{1}$$

where u_0^k is the in-plane displacement of the mid-plane of the layer, θ_x^k are rotations of normals to the mid-plane about the y axis (anticlockwise), w_0^k is the transverse displacement of the layer, $\bar{z}_k$ is the z coordinate of the mid-plane of each layer, with reference to the core layer mid-plane ($\bar{z}_c = 0$) and $k = t, b$ is the layer index. For the core layer, the HSDT displacement field is written as a Taylor series expansion of the displacements in the thickness coordinate:

$$\begin{aligned} u^c(x,y,z,t) &= u_0^c(x,t) + z\theta_x^c(x,t) + z^2 u_0^{*c}(x,t) + z^3\theta_x^{*c}(x,t) \\ w^c(x,y,z,t) &= w_0^c(x,t) + z\theta_z^c(x,t) + z^2 w_0^{*c}(x,t) \end{aligned} \tag{2}$$

where u_0^c is the in-plane displacement of the mid-plane of the layer, θ_x^c are rotations of normals to the mid-plane about the y axis (anticlockwise) w_0^c is the transverse displacement of the mid-plane of the layer, c is the layer index. The functions u_0^{*c}, w_0^{*c}, θ_x^{*c} and θ_z^c are higher-order terms in the series expansion, defined also in the mid-plane of the core layer.

The displacement continuity at the layer interfaces can be written as:

$$\begin{aligned} u^c(z = h_c/2) &= u^t(z = \bar{z}_t - h_t/2) \\ u^c(z = -h_c/2) &= u^b(z = \bar{z}_b + h_b/2) \\ w^c(z = h_c/2) &= w_0^t \\ w^c(z = -h_c/2) &= w_0^b \end{aligned} \tag{3}$$

where the coordinates of layer mid-planes are:

$$\begin{aligned}
\bar{z}_t &= h_c/2 + h_t/2 \\
\bar{z}_c &= 0 \\
\bar{z}_b &= -h_c/2 - h_b/2
\end{aligned} \tag{4}$$

Applying the continuity conditions one can eliminate the following unknowns:

$$\begin{aligned}
\theta_x^t &= \frac{2}{h_t}\left(u_0^t - u_0^c - \frac{h_c}{2}\theta_x^c - \frac{h_c^2}{4}u_0^{*c} - \frac{h_c^3}{8}\theta_x^{*c}\right) \\
\theta_x^b &= \frac{2}{h_b}\left(-u_0^b + u_0^c - \frac{h_c}{2}\theta_x^c + \frac{h_c^2}{4}u_0^{*c} - \frac{h_c^3}{8}\theta_x^{*c}\right) \\
\theta_z^c &= \frac{w_0^t - w_0^b}{h_c} \\
w_0^{*c} &= \frac{4}{h_c^2}\left(\frac{w_0^t + w_0^b}{2} - w_0^c\right)
\end{aligned} \tag{5}$$

The strain field is obtained from the displacement field as:

$$\left\{ \begin{array}{c} \varepsilon_{xx} \\ \varepsilon_{zz} \\ \gamma_{xz} \end{array} \right\}^k = \left[\begin{array}{cc} \frac{\partial}{\partial x} & 0 \\ \frac{\partial}{\partial z} & \frac{\partial}{\partial x} \\ 0 & \frac{\partial}{\partial z} \end{array} \right] \left\{ \begin{array}{c} u \\ w \end{array} \right\}^k \tag{6}$$

The linear strains associated with the assumed displacement field for the core layer are:

$$\begin{aligned}
\varepsilon_{xx}^c &= \frac{\partial u_0^c}{\partial x} + z\frac{\partial \theta_x^c}{\partial x} + z^2\frac{\partial u_0^{*c}}{\partial x} + z^3\frac{\partial \theta_x^{*c}}{\partial x} \\
\varepsilon_{zz} &= \theta_z^c + 2z w_0^{*c} \\
\gamma_{xz}^c &= \theta_x^c + \frac{\partial w_0^c}{\partial x} + z\left(2u_0^{*c} + \frac{\partial \theta_z^c}{\partial x}\right) + z^2\left(3\theta_x^{*c} + \frac{\partial w_0^{*c}}{\partial x}\right)
\end{aligned} \tag{7}$$

and the linear strains associated with the assumed displacement field for the face layers are:

$$\begin{aligned}
\varepsilon_{xx}^k &= \frac{\partial u_0^k}{\partial x} + z\frac{\partial \theta_x^k}{\partial x} - \bar{z}\frac{\partial \theta_x^k}{\partial x} \\
\gamma_{xz}^k &= \theta_x^k + \frac{\partial w_0^k}{\partial x}
\end{aligned} \tag{8}$$

2.2 Constitutive relations

Fibre-reinforced laminae are characterised as orthotropic, i.e., the material has three orthogonal planes of material symmetry. If the coordinate planes are parallel to the three orthogonal planes of material symmetry, the constitutive relations in matrix form may be written as:

$$\begin{Bmatrix} \varepsilon_{11} \\ \varepsilon_{22} \\ \varepsilon_{33} \\ \gamma_{23} \\ \gamma_{13} \\ \gamma_{12} \end{Bmatrix} = \begin{bmatrix} S_{11} & S_{12} & S_{13} & 0 & 0 & 0 \\ S_{12} & S_{22} & S_{23} & 0 & 0 & 0 \\ S_{13} & S_{23} & S_{33} & 0 & 0 & 0 \\ 0 & 0 & 0 & S_{44} & 0 & 0 \\ 0 & 0 & 0 & 0 & S_{55} & 0 \\ 0 & 0 & 0 & 0 & 0 & S_{66} \end{bmatrix} \begin{Bmatrix} \sigma_{11} \\ \sigma_{22} \\ \sigma_{33} \\ \sigma_{23} \\ \sigma_{13} \\ \sigma_{12} \end{Bmatrix} \tag{9}$$

where $[S]$ is the compliance matrix, defined in terms of the engineering parameters as:

$$[S] = \begin{bmatrix} \frac{1}{E_1} & -\frac{\nu_{21}}{E_2} & -\frac{\nu_{31}}{E_3} & 0 & 0 & 0 \\ -\frac{\nu_{12}}{E_1} & \frac{1}{E_2} & -\frac{\nu_{32}}{E_3} & 0 & 0 & 0 \\ -\frac{\nu_{13}}{E_1} & -\frac{\nu_{23}}{E_2} & \frac{1}{E_3} & 0 & 0 & 0 \\ 0 & 0 & 0 & \frac{1}{G_{23}} & 0 & 0 \\ 0 & 0 & 0 & 0 & \frac{1}{G_{13}} & 0 \\ 0 & 0 & 0 & 0 & 0 & \frac{1}{G_{12}} \end{bmatrix} \tag{10}$$

where the following reciprocal relation holds:

$$\frac{\nu_{ij}}{E_i} = \frac{\nu_{ji}}{E_j}, \qquad i, j = 1, 2, 3 \tag{11}$$

The nine independent engineering parameters necessary to characterise a general orthotropic material are: Young's moduli E_1, E_2 and E_3 in the principal material directions x_1, x_2 and x_3, respectively, shear moduli G_{23}, G_{13} and G_{12}, in planes (x_2, x_3), (x_1, x_3) and (x_1, x_2), respectively and the corresponding Poisson's ratios in the same planes ν_{23}, ν_{13} and ν_{12}.

Principal directions of orthotropy often do not coincide with coordinate directions which are geometrically natural to the solution of laminate problems. Thus it becomes necessary to apply coordinate transformations for stress and strain between the principal material directions (x_1,x_2,x_3) and the geometrically natural coordinate system (x,y,z). The coordinate transformations may be written in the following form [8]:

$$\left\{ \begin{array}{c} \sigma_{xx} \\ \sigma_{yy} \\ \sigma_{zz} \\ \sigma_{yz} \\ \sigma_{xz} \\ \sigma_{xy} \end{array} \right\} = \left[\begin{array}{cccccc} \cos^2\theta & \sin^2\theta & 0 & 0 & 0 & -2\sin\theta\cos\theta \\ \sin^2\theta & \cos^2\theta & 0 & 0 & 0 & 2\sin\theta\cos\theta \\ 0 & 0 & 1 & 0 & 0 & 0 \\ 0 & 0 & 0 & \cos\theta & \sin\theta & 0 \\ 0 & 0 & 0 & -\sin\theta & \cos\theta & 0 \\ \sin\theta\cos\theta & -\sin\theta\cos\theta & 0 & 0 & 0 & \cos^2\theta - \sin^2\theta \end{array} \right] \left\{ \begin{array}{c} \sigma_{11} \\ \sigma_{22} \\ \sigma_{33} \\ \sigma_{23} \\ \sigma_{13} \\ \sigma_{12} \end{array} \right\} \tag{12}$$

where θ is the angle between the beam x axis and principal material direction x_1.

Finally, the constitutive equation can be written in the (x, y, z) reference coordinate system as:

$$\{\sigma\}_{(x,y,z)} = \left[\bar{C}\right] \{\varepsilon\}_{(x,y,z)} \tag{13}$$

where $\left[\bar{C}\right] = [T]\,[C]\,[T]^T$ is the stiffness matrix and $[T]$ is the transformation matrix in Equation (12) and $[C] = [S]^{-1}$.

For the present sandwich beam model, the following conditions are a consequence of the assumed displacement field: for the core $\varepsilon^c_{yy} = \gamma^c_{xy} = \gamma^c_{yz} = 0$ and for the face layers $\varepsilon^k_{yy} = \varepsilon^k_{zz} = \gamma^k_{xy} = \gamma_{yz} = 0^k$, with $k = t, b$. In terms of constitutive relations for the beam model, after imposing these conditions we obtain:

$$\left\{ \begin{array}{c} \sigma_{xx} \\ \sigma_{xz} \end{array} \right\}^k = \left[\begin{array}{cc} \bar{C}^k_{11} & 0 \\ 0 & \bar{C}^k_{55} \end{array} \right] \left\{ \begin{array}{c} \varepsilon_{xx} \\ \gamma_{xz} \end{array} \right\}^k \tag{14}$$

with $k = t, b$, and for the core layer:

$$\left\{ \begin{array}{c} \sigma_{xx} \\ \sigma_{zz} \\ \sigma_{xz} \end{array} \right\}^c = \left[\begin{array}{ccc} \bar{C}^c_{11} & \bar{C}^c_{13} & 0 \\ \bar{C}^c_{13} & \bar{C}^c_{33} & 0 \\ 0 & 0 & \bar{C}^c_{55} \end{array} \right] \left\{ \begin{array}{c} \varepsilon_{xx} \\ \varepsilon_{zz} \\ \gamma_{xz} \end{array} \right\}^c \tag{15}$$

Explicit expressions can be obtained for the stiffness entries of these constitutive relations in terms of engineering constants, but they are not included herein for the sake of brevity.

The definition of constitutive relations of a laminate is usually made in terms of stress resultants [9]. These forces and moments for the present model are defined separately for the core and the laminated face layers [7].

2.3 Finite Element Formulation

Using the principle of minimum potential energy:

$$\Pi_k = U_k + W \tag{16}$$

where Π_k is the potential energy of each layer and U_k and W are, respectively, the energy associated with strains in each layer and the work done by externally applied loads:

$$\begin{aligned} U_k &= 1/2 \int_\Omega \left\{\varepsilon^k\right\}^T \left\{\sigma^k\right\} d\Omega \\ W &= -\left(\int_\Omega \{d\}^T \{f_b\}\, d\Omega + \int_S \{d\}^T \{f_s\}\, dS + \{d\}^T \{f_c\} \right) \end{aligned} \tag{17}$$

where $\left\{\varepsilon^k\right\}$ and $\left\{\sigma^k\right\}$ are the components of the strain and stress fields, respectively, $\{d\}$, $\{f_b\}$, $\{f_s\}$ and $\{f_c\}$ are the vector of degrees of freedom, the vector of applied loads in the body, the vector of surface tractions and the vector of concentrated forces, respectively. Finally, Ω and S represent, respectively, the volume and surface domains of the beam.

The displacement field can be given as

$$\left\{u^k\right\} = [Z]^k \{d\} \tag{18}$$

where the vector of degrees of freedom, after reducing the unknowns through the continuity conditions in Equations (3) and (5) is:

$$\{d\} = \left\{ \begin{array}{cccccccccc} u_0^b & w_0^b & u_0^c & w_0^c & \theta_x^c & u_0^{*c} & \theta_x^{*c} & u_0^t & w_0^t \end{array} \right\}^T \tag{19}$$

Carrying on the integration in the thickness direction in Equation (17) and substituting the results in Equation (16), one obtains the variational equation of motion for the sandwich beam, whose solution was obtained through the finite element model using a three-nodded element with 9 DOF per node with:

$$\{d^e\} = \sum_{i=1}^{NN} [N_i] \{d_i^e\} = [N] \{a^e\} \tag{20}$$

where NN is the number of nodes in the element and $[N]$ contains the C^0 quadratic shape functions.

The strains are related to the element DOF through:

$$\begin{aligned} \left\{\varepsilon_m^e\right\}^k &= \sum_{i=1}^{NN} \left[B_{mi}\right]^k \{d_i^e\} = \left[B_m\right]^k \{a^e\} \\ \left\{\varepsilon_b^e\right\}^k &= \sum_{i=1}^{NN} \left[B_{bi}\right]^k \{d_i^e\} = \left[B_b\right]^k \{a^e\} \\ \left\{\varepsilon_s^e\right\}^k &= \sum_{i=1}^{NN} \left[B_{si}\right]^k \{d_i^e\} = \left[B_s\right]^k \{a^e\} \end{aligned} \tag{21}$$

where $[B_m]$, $[B_b]$ and $[B_s]$ are strain matrices that can be obtained from the shape functions and their derivatives, and are calculated on a layer-by-layer basis.

It is now possible to build the equilibrium equation in matrix form:

$$[K^e]\{a^e\} = \{F^e\} \tag{22}$$

Where $[K^e]$ is the stiffness matrix of the element given by:

$$[K^e] = \sum_{k=c,t,b} \int_{-1}^{+1} \Big([B_m^e]^{kT} [D_m]^k [B_m^e]^k + [B_b^e]^{kT} [D_c]^k [B_m^e]^k + [B_m^e]^{kT} [D_c]^k [B_b^e]^k + [B_b^e]^{kT} [D_b]^k [B_b^e]^k + [B_s^e]^{kT} [D_s]^k [B_s^e]^k \Big) \det[J]\, d\xi \tag{23}$$

where ξ is the natural coordinate of the element and J is the Jacobian of the transformation. $[D_m]$, $[D_c]$, $[D_b]$ and $[D_s]$ are the constitutive matrices with the membrane, coupled, bending and shear contributions, respectively. Shear locking was avoided using selective integration in the construction of the stiffness matrices.

3 Validation

The goal is to validate the results obtained with the present beam model with experimental and 3D FEM results obtained by Teixeira de Freitas et al. [3], for the application of a SPS system in Dutch bridge decks.

The beam specimens characteristics used in these tests are presented in Table 1:

Specimen	h_b (mm)	h_c (mm)	h_t (mm)
S12305	12	30	5
S12155	12	15	5
S12206	12	20	6
S12306	12	30	6
S10306	10	30	6

Table 1: Specimen characteristics.

Steel Grade S355 was selected for both steel faces, with properties $E = 210$ GPa and $\nu = 0.3$. The sandwich core is polyurethane (solid polymer) with a mass density of 1150 kg/m^3 and a Poisson's ratio of 0.36, manufactured by Elastogran GmbH. The core material was first tested by Teixeira de Freitas et al. [3] for the three temperatures and the mean values obtained are shown in Table 2.

Temperature	E (MPa)	σ_{ced} (MPa)
-10 $°C$	1049	22
RT	721	25
50 $°C$	471	17.7

Table 2: Young's modulus (E) and yield stress (σ_{ced}) for the core material.

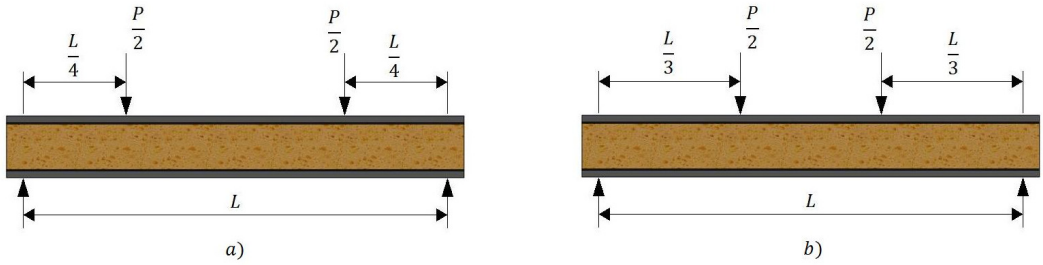

Figure 2: Four point bending tests configuration in accordance with ASTM-C393: a) Short beams loading; b) Long beams loading

3.1 Experimental Procedure

The tests were conducted under three different temperatures (-10 $°C$, Room Temperature (RT) and +50 $°C$), in accordance with ISO-527 (1996) [10], in order to test the core behaviour when subject to real conditions.

For these four point bending tests, two types of load configuration were used: short and long beams [3]. The short beam load configuration was one quarter point loading with 400 mm support span and 200 mm load span. The long beam load configuration was one third point loading with 750 mm support span and 250 mm load span. Figure 2 shows both load configurations.

3.2 Results and discussion

The bending stiffness values K, ($K = load/displacement$), obtained for the short and long beam configurations at -10 $°C$, room temperature (RT) and 50$°C$ are presented in Table 3.

The results from 3D FEM were obtained by Teixeira de Freitas et al. [3] using ABAQUS [11], where both faces and core were modelled using C3D20R three dimensional 20-node continuum (solid) elements with reduced-integration.

It can be concluded that for the long beam configuration the beam element results are closer to the experimental values than the 3D FEM results, except for the 50 °C situation. This behaviour is possibly due to viscoleastic effects of the polyurethane at that temperature.

In the short beam configuration, where the shear effects are more significant, devi-

	-10 °C			RT			+50 °C		
	Exp.	3D FEM	Present	Exp.	3D FEM	Present	Exp.	3D FEM	Present
Short beam									
S12305	39.4	36.4	32.3	32.3	29.1	24.4	20.2	22.5	18.2
S12155	28.2	23.2	22.7	22.0	19.7	18.2	9.0	16.2	14.3
S12206	38.3	29.8	27.0	29.6	24.5	21.3	13.3	19.5	16.1
S12306	46.2	38.6	33.3	37.1	30.6	25.6	19.0	23.6	18.9
S10306	42.7	34.0	29.4	34.2	26.6	22.2	16.2	20.1	16.1
Long beam									
S12305	8.8	8.1	8.9	7.6	6.8	7.1	4.5	5.3	5.4
S12155	4.6	4.2	5.0	4.2	3.8	4.3	2.0	3.2	3.5
S12206	7.0	6.1	6.8	6.2	5.2	5.7	2.9	4.2	4.4
S12306	9.9	8.9	9.6	8.5	7.3	7.6	4.7	5.7	5.7
S10306	9.4	8.0	8.7	8.0	6.6	6.9	4.3	5.1	5.2

Table 3: Results for bending stiffness K (kN/mm)

ations of both numerical models are higher than in the short beam case. However, in this case, the 3D FEM results appear to be closer to the experimental ones.

The longitudinal strains distribution of specimens S12305 and S12155 along the thickness of the sandwich are shown in Figures 3 and 4. From the analysis of these figures it can be concluded that for the long beam configuration all the models are in accordance. For the short beam configuration the beam element results when compared to the 3D element evidence that in 3D FEM the shear effects are more significant in the specimen S12305, since its core is twice as thick as the S12155 specimen.

4 Conclusion

For long beam configuration the beam element presented here is quite accurate and in accordance with the results obtained using the three-dimsnional finite element method. For the short beam configuration, where shear effects are more noticeable, as expected the three-dimensional finite element results seem to be closer to the experimental ones. The viscolelastic effects of the polyurethane core, especially at 50 °C, also leads to great discrepancies between the experimental and the numerical results. Better understanding is still needed concerning the modelling of short sandwich beams with beam elements and aspects that can bridge the gap between the beam model and the three-dimensional strain distribution will be further studied.

References

[1] H.G. Allen, "Analysis and Design of Structural Sandwich Panels", Pergamon Press, 1969.

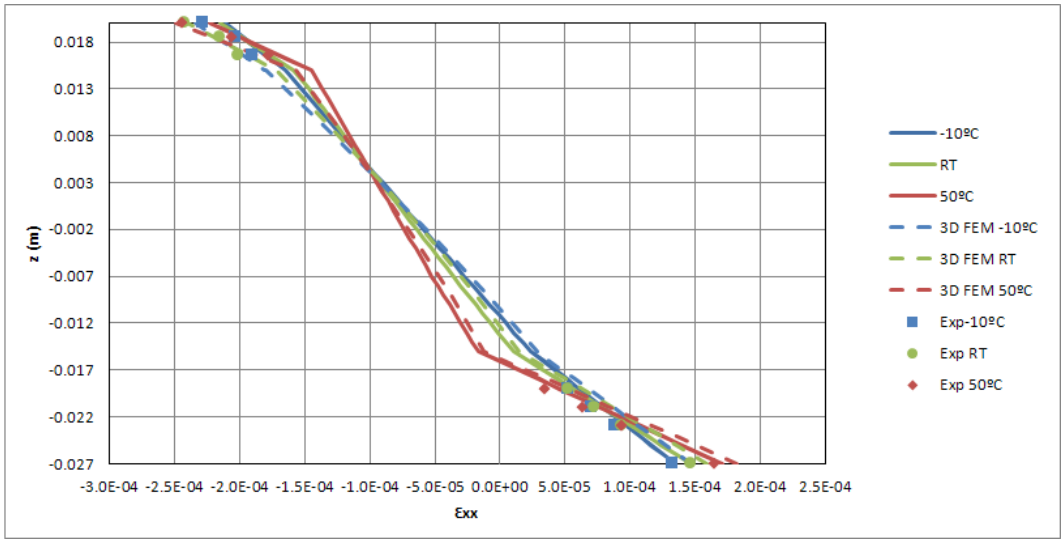

(a)

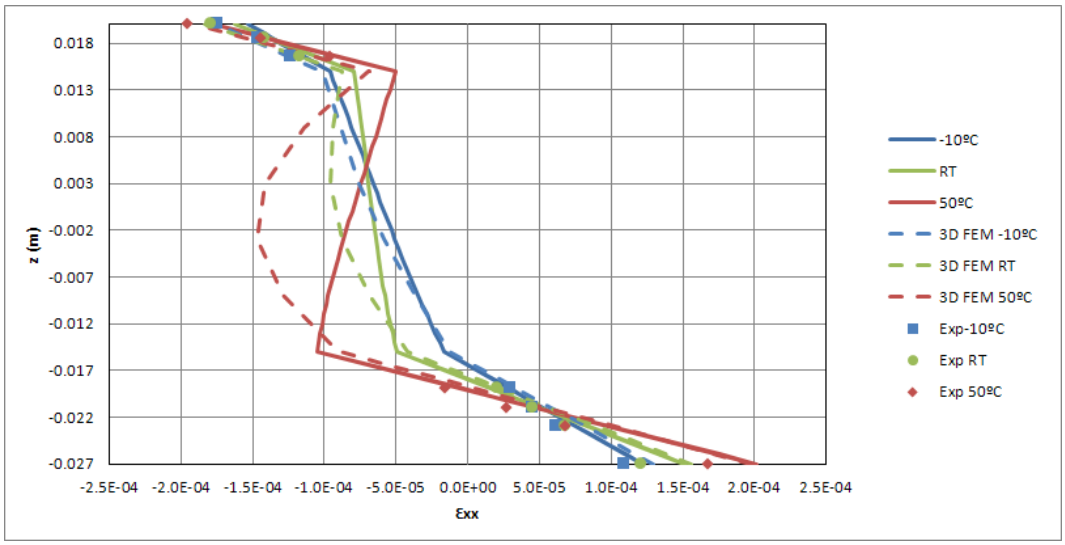

(b)

Figure 3: Longitudinal strain, ε_{xx}, for S12305 specimen in mid-span section in (a) Long beam and (b) Short beam configurations.

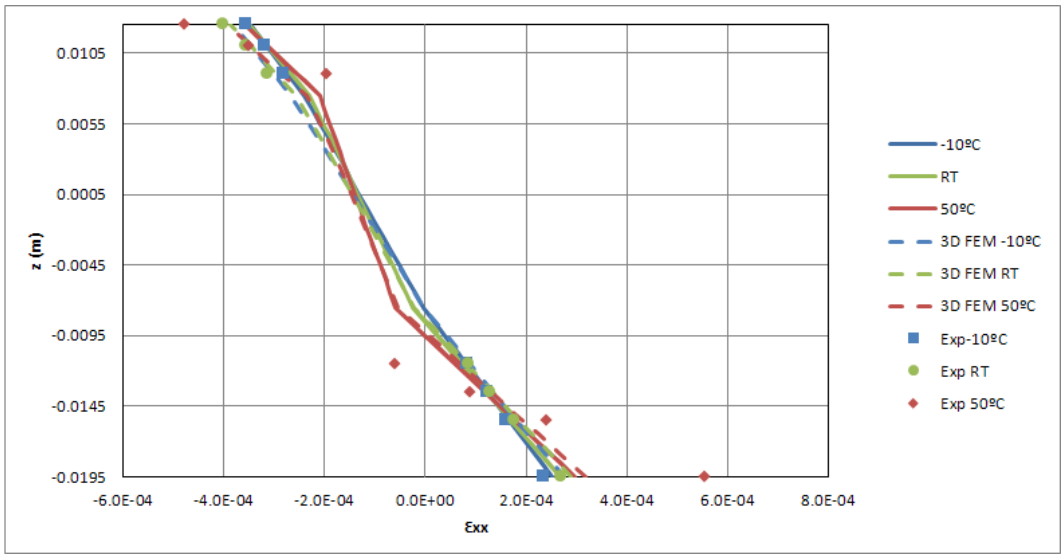

(a)

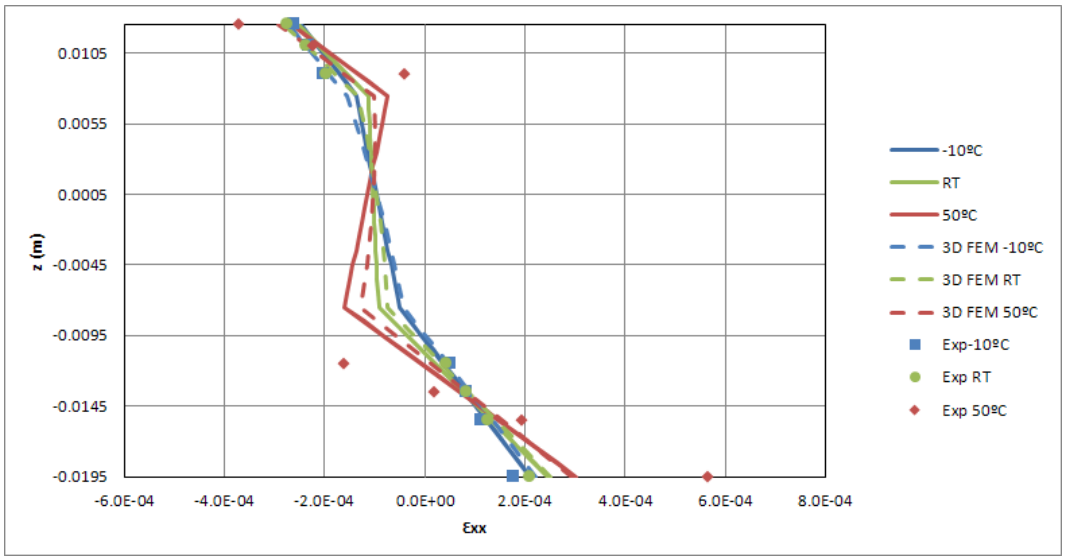

(b)

Figure 4: Longitudinal strain, ε_{xx}, for S12155 specimen in mid-span section in (a) Long beam and (b) Short beam configurations.

[2] J.M. Davies, "Lightweight Sandwich Construction", Blackwell Publishing, 2001.

[3] S. Teixeira de Freitas, H. Kolstein, F. Bijlaard, "Sandwich System for Renovation of Orthotropic Steel Bridge Decks", Journal of Sandwich Structures and Materials, 13(3), 279-301, 2011.

[4] Vincent, R., A. Ferro, A New Orthotropic Bridge Deck: "Design, Fabrication and Construction of the Shenley Bridge Incorporating an SPS Orthotropic Bridge Deck", In 2004 Orthotropic Bridge Conference, Sacramento, California, USA, 2004.

[5] M. Feldmann, G. Sedlacek, A. Geler, "A System of Steel-Elastomer Sandwich Plates for Strengthening Orthotropic Bridges Decks", Mechanics of Composite Materials, 43(2), 183-190, 2007.

[6] ASTM-C393, "C393-06: Standard Test Method for Core Shear Properties of Sandwich Constructions by Beam Flexure", 2006.

[7] A.L. Araújo, C. M. Mota Soares, C. A. Mota Soares, "Finite Element Model for Hybrid Active-Passive Damping Analysis of Anisotropic Laminated Sandwich Structures", Journal of Sandwich Structures and Materials, 12, 397-419, 2010.

[8] J.N. Reddy, "Mechanics of Laminated Composite Plates and Shells: Theory and Analysis", 2nd Edition, CRC Press, Boca Raton, 2004

[9] A.L. Araújo, C.M. Mota Soares, J. Herskovits, P. Pedersen, "Development of a Finite Element Model for the Identification of Mechanical and Piezoelectric Properties Through Gradient Optimization and Experimental Vibration Data", Composite Structures, 58, 307-318, 2002.

[10] ISO-527, "EN ISO 527:1996 Plastics - Determination of Tensile Properties", 1996.

[11] ABAQUS, "Analysis User's Manual Version 6.5", Hibbit, Karlsson and Sorensen Inc.,RI, USA, 2005.